J Therm Anal Calorim (2012) 107:447–452
DOI 10.1007/s10973-011-1856-3

Imaging and diffusion structural diagnostics of silicon carbide-based composites and fibers

H. Tatlisu · V. Balek · I. N. Beckman · N. Kardjilov · A. Hilger · H. Rauch

Received: 30 December 2010 / Accepted: 10 August 2011 / Published online: 23 August 2011

Abstract The aim of this study is to characterize the microstructure and high temperature induced structural changes within fiber reinforced silicon carbide (SiC_f/SiC) composites by means of non-destructive techniques. In order to understand their properties, the characterization of the microstructure of SiC_f/SiC composites is the crucial issue. Porosity within composites is unavoidable with currently available manufacturing processes, and reduces significantly the life time and performance of the composites under harsh environments. Moreover, the internal pores, created in the manufacturing process cause the degradation most of the outstanding properties such as thermal conductivity, mechanical properties at high temperature, and radiation stability. Cold neutron tomography and diffusion structural diagnostic techniques were applied in the investigation of the microstructure of SiC_f/SiC composites to gain complementary information. One of the main obstacles to using these composites in fusion technology and other applications are a change of the porous structure and a swelling at high temperatures and in a severe radiation environment. Cold neutron tomography enables visualization of the microstructure of the composite and consequently the pore distributions within the SiC_f/SiC composite were observed with a suitable resolution. The diffusion structural diagnostic technique was used to characterize the thermal behavior of SiC_f/SiC composites on heating up to 1300 °C.

Keywords Emanation · Fusion technology · Neutron tomography · SiC_f/SiC inner microstructure · Thermal analysis

H. Tatlisu (✉) · H. Rauch
Institute of Atomic and Subatomic Physics (Formerly Atominstitute), Vienna, Austria
e-mail: tatlisu@ati.ac.at

V. Balek
Research Centre Institute Řež Ltd, CZ-25068 Řež, Czech Republic

I. N. Beckman
Chemical Faculty, Moscow State University, Moscow, Russia

N. Kardjilov · A. Hilger
Helmholtz Zentrum Berlin (Formerly Hahn-Meitner Institut), Berlin, Germany

Introduction

SiC_f/SiC composites developed for fusion technology, gas turbine, and aerospace industry, and advanced fission applications are currently under study. The appealing properties of such a SiC_f/SiC composite are mainly its high strength at elevated temperature, low density, light weight, and inherent radiation tolerance make it ideal for the replacement of metals [1–3]. These promising performances of a SiC_f/SiC composite make it a favorite candidate material for structural applications in fusion technology.

SiC_f/SiC composite is composed of silicon carbide fiber (14 μm diameter of fibers) bundles. These bundles are woven in three dimensional textures and embedded in a silicon carbide matrix. Hi-Nicalon and Nicalon (Nippon Carbon Company, Japan) SiC fibers based on SiC_f/SiC composites have been investigated in this study. Hi-Nicalon SiC fiber (2.74 g/cm^3) consists of nearly of 62 wt% Si, 37 wt% C, and 0.5 wt% O while Nicalon SiC fiber (2.55 g/cm^3) consists of 57 wt% Si, 32 wt% C, and 12 wt% O. SiC_f/SiC composite was manufactured by SNECMA using a chemical vapor infiltration (CVI) method, which is widely used for fabrication of ceramic matrix composites. CVI is

an efficient technique to manufacture high quality composite but a slow process, and with this method unavoidable residual pores remain in the SiC matrix [4, 5]. Despite a repeat of the CVI process, the residual porosity within the composite is between 15 and 20%. The porosity is a critical technological issue for the use of the ceramic matrix composites, since porosity causes degradation of the thermal conductivity, mechanical properties at high temperature, and radiation stability. Importantly, the porosity tends to affect importantly the initiation of matrix cracks. Pore sizes can vary over a wide range of micro-, meso-, and macropores. One of the main obstacles to using this composite in fusion technology and other applications are the change of porous structure markedly at high temperature. Improvement of applicability of the SiC_f/SiC composite demands a comprehensive understanding of the pore structure.

Scanning electron microscopy (SEM), cold neutron tomography, and emanation thermal analysis (ETA) techniques have been utilized for the investigation of the microstructure in and on the composites. Cold neutron tomography and ETA are two powerful non-destructive techniques that are used to characterize pore structure in porous materials on a micrometer length scale. Neutron tomography is a useful technique for the analysis of the macroscopic inner structure of the SiC_f/SiC composite with a spatial resolution up to 100 μm [6, 7].

Temperature induce performance evaluation of the microstructure has been performed up to 1300 °C using the ETA technique.

Imaging of the composite structure

Non-destructive imaging techniques are essential to visualize the structure and possible defects within the SiC_f/SiC composites and to analyze any structural changes before and after any process applied to the composites. Figure 1 shows a surface analysis on the SiC_f/SiC composite performed by SEM method. SEM is a surface scanning method and allows the determination of the pore size in the localized area. The inherent pores with different sizes can easily be seen on the SEM image in Fig. 1 where two large and small pores are marked by the arrows. The inset on the left top of the image shows the SiC fibers (14 μm) that were embedded into SiC matrix material using the CVI method.

Pore morphology within the composite cannot be investigated using direct imaging methods such as SEM and TEM. In order to visualize the pores, which are located within the composite, neutron imaging has been implemented. The porous structure distribution in the sample has been determined by cold neutron tomography.

The neutron imaging method is based on the neutron beam attenuation by the elements within a sample. Due to

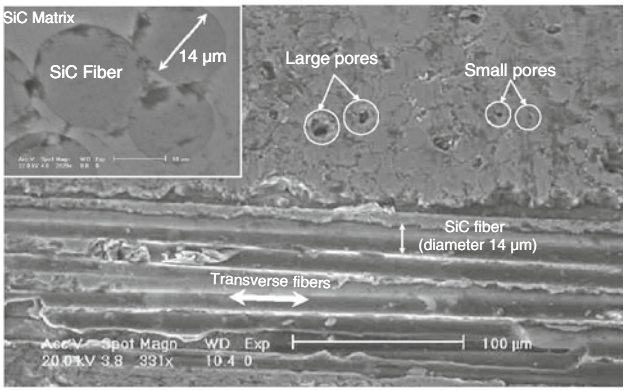

Fig. 1 Scanning electron microscopy image from the side of a SiC_f/SiC composite

the neutron attenuation differences between different elements/isotopes, the interior structure of a sample can be visualized. The neutron attenuation through a sample depends on the neutron beam energy which influences strongly the visualization of the sample interior. Cold neutrons have an advantage over thermal neutrons because the cold neutrons interact stronger with the sample and provide better contrast for small amounts of material.

Neutron tomography measurements using a cold neutron beam of wavelength between 2 and 12 Å with a maximum at 3 Å have been performed at the neutron imaging setup CONRAD at the Helmholtz Zentrum Berlin (HZB). A ^{6}LiZnS scintillator with a 16-bit cooled CCD (Charge Coupled Device) camera having 2048 × 2048 pixels was used for cold neutron imaging. The spatial resolution of a neutron attenuation image is directly based on the beam collimation. The beam collimation is expressed by the *L/D* ratio, where *L* is the distance between aperture and sample and *D* is the diameter of the aperture. The SiC_f/SiC composite was investigated at the collimation ratio of 200 and spatial resolution of 200 μm. The neutron flux at the sample position, which affects the exposure time of the sample for an image, was approximately 10^7 n/cm^{2}s [8, 9].

SiC_f/SiC composite is quite difficult to investigate with neutron tomography due to the poor contrast between fibers and matrix. However, this is not a main concern for our

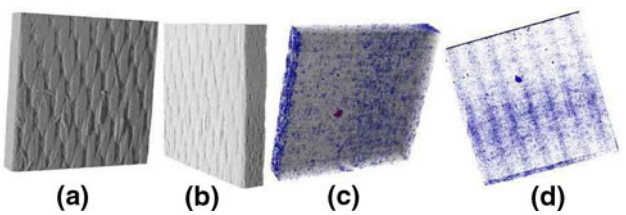

Fig. 2 3D reconstructed neutron tomography images of the Hi-Nicalon fibers based on SiC_f/SiC composite with different opacity levels. **a**, **b** images taken without segmentation. **c**, **d** images taken from the different views with segmentation. *Blue parts* show the pores

investigation, because porosity is the main issue. The macroscopic pore distribution within SiC_f/SiC composite was revealed after reconstruction of the 3D micro-structure of a SiC_f/SiC composite using non-destructive cold neutron tomography technique, as seen in Fig. 2. The Octopus software for the 3D image reconstruction and the 3D viewer software VG Studio® for 3D image visualization were employed [10]. Fiber bundles consisting of SiC fibers in woven texture can clearly be seen in Fig. 2a. Pores and cracks on the surface could be visualized from the side view of the composite as seen in Fig. 2b. The silicon carbide matrix cannot be distinguished from the silicon carbide fibers because both consist of the same elements. Only separation of the pores from the composite has been obtained, i.e., the contrast changes take place at porosity and the rest of the composite. The porosity characteristic of the composite can be clearly seen in Figs. 2c, d. In 3D visualization, the opacity level is changed to highlight the inhomogeneities within the composite.

ETA method and experimental conditions

An ETA is performed by measuring the radon release rate from samples previously labeled by trace amounts of ^{228}Th and ^{224}Ra radionuclides [11–13].

Atoms of radon, ^{220}Rn, are incorporated by the recoil energy (85 keV atom^{-1}) of spontaneous α-decay of the parent radionuclides ^{228}Th and ^{224}Ra, respectively. It was supposed that ^{228}Th and ^{224}Ra do not migrate in the solid at the temperatures used for the ETA measurements. The ^{228}Th radionuclide (half-life 1.9 years) adsorbed on the sample from an acetone solution represents a quasi-permanent source of ^{220}Rn atoms (half-life 55 s), and consequently the ETA can be used for the characterization of thermal behavior of materials during heating to elevated temperatures and even during repeated heating.

A labeled SiC based sample with a size of 3 × 3 × 2 mm was situated in a furnace and heated in the temperature range from 30 to 1300 °C at a heating rate of 6 °C/min in a flow of argon. The constant flow of the gas (flow rate 50 mL/min) took the radon released from the sample into the measuring chamber for radon radioactivity. The specific activity of the sample was 10^5 Bq per gram. The resulting ETA curve is presented as the temperature dependence of the radon release rate E (in relative units); $E = A_\alpha/A_{total}$, where A_α is α-radioactivity of radon released in unit time from the labeled sample, and A_{total} is the total γ-radioactivity of the labeled sample. The A_{total} value is proportional to the rate of radon formation in the sample. Semiconductor and NaI(Tl) detectors were used for the α–and γ-radioactivity measurements, respectively .

Modeling and evaluation of ETA results

The mobility of radon tracers used in the diffusion structural diagnostics of the materials can be described by the theory proposed recently by Beckman et al. [14]. The temperature dependence of the radon release rate was characterized by the functions E_D and $\Psi(T)$. The $E(T)$ function can be expressed as

$$E(T) = E_D(T) \cdot \Psi(T) \quad (1)$$

where E_D is the radon release rate due to diffusion along structure irregularities, serving as radon diffusion paths, and $\Psi(T)$ is the function which describe the temperature

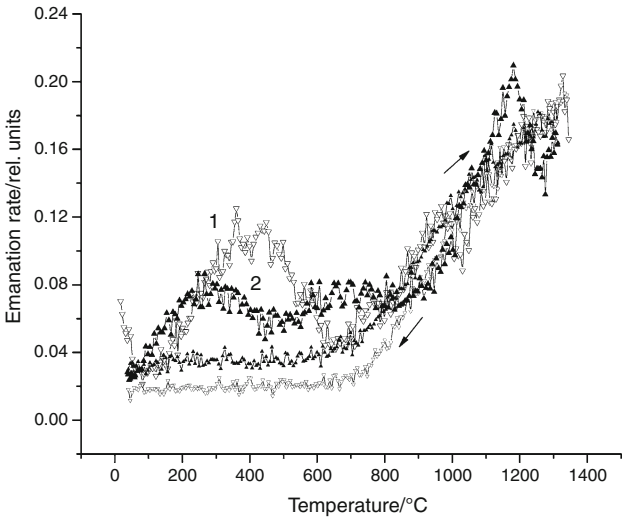

Fig. 3 ETA results of the SiC_f/SiC composite and the Nicalon SiC fiber on heating and cooling. *Curve 1* corresponds to the SiC_f/SiC composite, *curve 2* corresponds to the SiC fiber

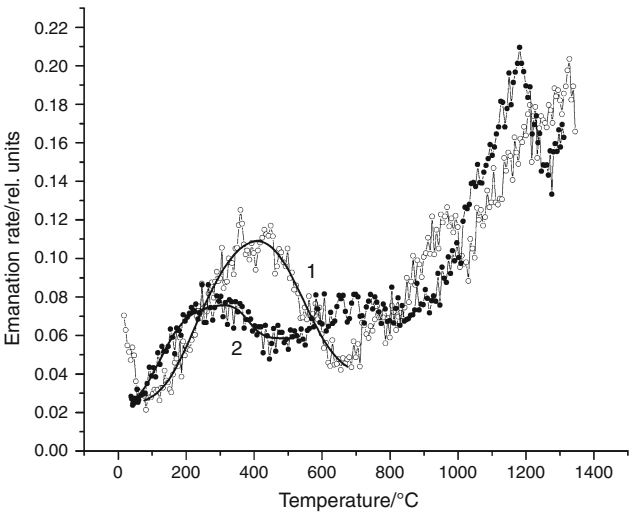

Fig. 4 ETA results of the SiC_f/SiC composite and the Nicalon SiC fiber on heating. *Curve 1* corresponds to the SiC_f/SiC composite, *curve 2* corresponds to the SiC fiber

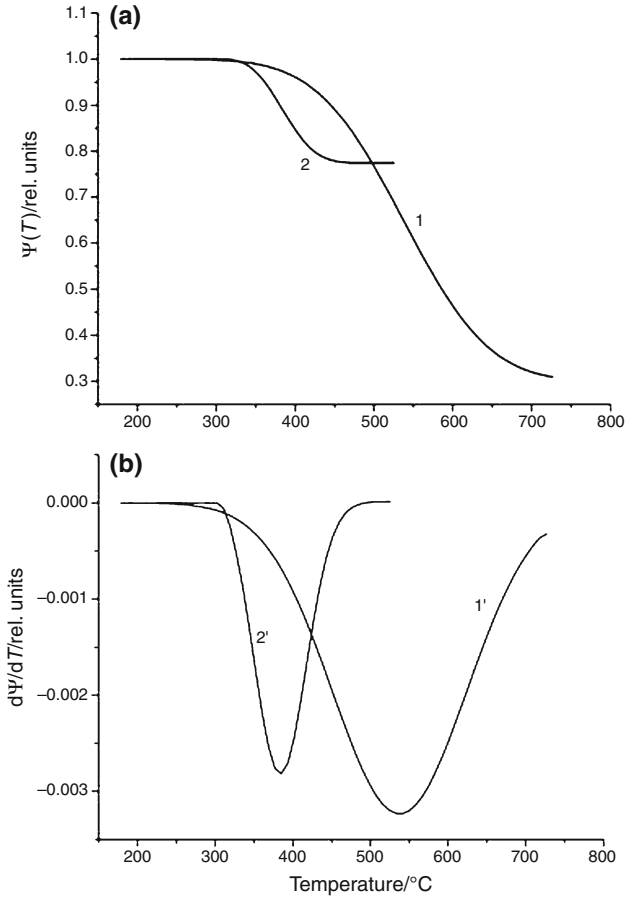

Fig. 5 **a** Temperature dependences of Ψ(T) functions that characterize of the annealing of near surface microstructure irregularities within SiC_f/SiC composite (*Curve 1*) and Nicalon SiC fiber (*Curve 2*). **b** Temperature dependences of Ψ(T)/dT functions describing the annealing of near surface layer irregularities of SiC_f/SiC composite (*Curve 1*) and Nicalon SiC fiber (*Curve 2*)

dependence of changes in the number of radon diffusion paths.

The maximal penetration depth of ^{220}Rn recoiled atoms into SiC based samples was 83.6 nm, as determined by the TRIM code [15]. Taking into account the average diffusion length of radon $L_D = (D/\lambda)^{1/2}$, where D is the radon diffusion coefficient and $\lambda = 0.0127\ s^{-1}$ is the radon decay constant. It was supposed that within the SiC sample heated to 1000 °C contained atoms of radon to a depth of 130 nm from the surface. It was assumed that radon migrates along several independent paths, such as micropores and intergranular space, as well as interface boundaries between fibers and matrix. The high amount of ^{220}Rn situated next to the surface ensured the high sensitivity of ETA to microstructure in the near surface layers of SiC fiber based composites.

In addition, the temperature dependence of the radon release obtained by the DSA was used for the evaluation of the permeability of porous solids and microstructure development characterization on heating of the samples.

The following equations were used to evaluate ETA data based on the mathematical model and the radon release rate due to diffusion was expressed as

$$E_D(T) = A\left[\frac{1}{k_{D0}\exp\left(-\frac{Q_D}{RT_0}\right)+\lambda_{Rn}} - \frac{1}{k_{D0}\exp\left(-\frac{Q_D}{RT}\right)+\lambda_{Rn}}\right] \quad (2)$$

where λ_{Rn} is the decay constant of ^{220}Rn, $A = \lambda_{Ra}C_{Ra}$ is a coefficient of concentration transformation, $\lambda_{Ra} = 2.2035 \times 10^{-6}\ s^{-1}$. The desorption rate constant (k_D) of radon depending on temperature according to an Arrhenius relationship is given by $k_D = k_{D0}\exp(-Q_D/RT)$, where k_{D0} is a coefficient of radon desorption, Q_D is the activation energy of radon desorption, $R = 8.3096\ J\ mol^{-1}\ K^{-1}$ is the molar gas constant.

For the description of changes in the number of the radon diffusion paths the following temperature dependence was used:

$$\Psi(T) = 1 - \frac{\kappa}{2}\left[1 + \mathrm{erf}\frac{1-\frac{T_m}{T}}{\frac{\Delta T\sqrt{2}}{T}}\right] \quad (3)$$

where erf is the sign for the integral Gauss function, T_m is the temperature of maximal rate of annealing of the defects which serve as radon diffusion paths, ΔT is the temperature interval of the respective solid state process, and κ is a parameter describing the contribution of the respective solid state process to the change in the number of the radon diffusion paths.

Table 1 Results of diffusion structural diagnostics used for the characterization of transport properties and microstructure annealing of the Nicalon SiC fiber based composite and fibers

SiC based sample	Heating temperature interval/°C 20–400		Cooling temperature interval/°C 1400–20		Microstructure annealing characteristics on sample heating		
	Radon mobility characteristics		Radon mobility characteristics				
	Q/kJ mol^{-1}	K_D/s^{-1}	K_D/s^{-1}	Q/kJ mol^{-1}	T_{onset}/°C	T_{final}/°C	T_{max}/°C
SiC_f/SiC composite	34	24	187	102	260	730	560
Nicalon fibers	4.8×10^{-4}	2.6×10^{3}	2.0×10^{3}	97	300	490	385

Results

Figures 3 and 4 depict the ETA curves obtained during heating of Nicalon SiC fiber and SiC_f/SiC composites in argon. The increase of the slope of the ETA curve was observed in the range 50–200 °C on heating the sample in argon; it indicated the enhanced radon mobility in the SiC_f/SiC composite. Another enhancing effect on radon mobility and radon permeability in the SiC_f/SiC composite was observed in the range 700–1300 °C perhaps due to a bulk diffusion mechanism as a controlling mechanism for the radon release from the sample.

The decrease of the emanation rate, E, observed in the temperature range 380–700 °C for the SiC_f/SiC composite, characterizes the annealing of structure irregularities in the near surface layers. In order to quantitatively characterize the annealing process, the mathematical model was used assuming that radon migration takes place by diffusion in open pores, intergranular space or interface boundaries.

Curve 2 in Figs. 3 and 4 show ETA results which characterize the thermal behavior of the Nicalon SiC fiber. Curve 1 in Figs. 3 and 4 show ETA results describing the thermal behavior of the SiC_f/SiC composite. The differences between the thermal behavior of the SiC_f/SiC composite and the SiC fiber can be deduced from the comparison of the curves 1 and 2. The effect observed on SiC fiber in the range 200–900 °C may characterize the microstructure changes of the corresponding to face transition of silica, present in the sample Si–C–O (Nicalon CG), and crystallization process leads to the decreasing of the emanation rate of the SiC fiber observed above 1200 °C, as seen in Fig. 4.

Equations 2 and 3 were used for the mathematical modeling and determination of annealing processes. The temperature dependence of $\Psi(T)$ functions was calculated using Eq. 3. Figure. 5a shows the temperature dependence of the $\Psi(T)$ functions which describe the annealing of surface and in the vicinity of the surface microstructure irregularities in the composite and fiber. The beginning of the annealing temperature of radon diffusion was determined as 300 °C. In order to determine the maximum rate of the model process, the Eq. 3 was calculated as first derivative of the curve 1 and 2 in the Fig. 5a and the derived results are shown in the Fig. 5b.

The values of parameters used in the mathematical models are listed in Table 1.

Conclusions

Although SiC_f/SiC composite is a very weak neutron attenuating sample, cold neutron tomography showed a big potential in structure analysis of this kind of composites. The pore distribution within the SiC_f/SiC composite was clearly visualized using cold neutron tomography. However, the majority of the pores within the composite are oriented along the fiber orientation. Fiber reinforced SiC_f/SiC composite contains significant porosity and it should be taken into consideration for fusion applications. Cold neutron tomography provides direct useful information on the inner microstructure of the SiC_f/SiC composite which is the crucial point for the manufacture of a stable composite. Moreover, it is recommended to determine porosity tolerance limits of each application for such kind of composites to decide its applicability.

ETA was used in the diffusion structural diagnostic for characterization of thermal behavior of SiC_f/SiC composite and the respective SiC fibers on heating in argon atmosphere. The annealing of near surface structure irregularities was observed on heating up to 700 °C and evaluated by means of a mathematical model, assuming that the structure irregularities served as diffusion paths for radon. Transport properties of the investigated materials were characterized from the evaluated radon mobility. The diffusion structural diagnostic based on ETA results made possible to characterize the differences in the microstructure development in studied SiC fiber and SiC_f/SiC composite on heating in temperature range from 700 to 1300 °C and to evaluate the transport properties of the respective samples heated to 1300 °C.

Acknowledgements This study has been supported by the Ministry of Education, Youths and Sports of the Czech Republic (Project No. MSM 2672244501) and by the European Communities under the contract of Association between EUATOM/ÖAW.

References

1. Katoh Y, et al. Current status and critical issues for development of SiC composites for fusion applications. J Nucl Mater. 2007;367–370:659–71.
2. Nozawa I, et al. Recent advances and issues in development of silicon carbide composites for fusion applications. J Nucl Mater. 2009;386–388:622–7.
3. Tatlisu H, et al. Structural investigation of SiC_f/SiC composites. Mater Struct. 2008;15:13–6.
4. Ortona A, et al. SiC-SiC_f CMC manufacturing by hybrid CVI-PIP techniques: process optimization. Fusion Eng Des. 2000;51–52:159–63.
5. Igawa N, et al. Fabrication of SiC fiber reinforced SiC composite by chemical vapor infiltration for excellent mechanical properties. J Phys Chem Solids. 2005;66:551–4.
6. Strobl M, et al. Advances in neutron radiography and tomography. J Phys D Appl Phys. 2009;42:243001.
7. Banhart J, et al. X-ray and neutron imaging—complementary techniques for materials science and engineering. Int J Mater Res. 2010;2010(09):1069–79.
8. Kardjilov N, et al. Industrial applications at the new cold neutron radiography and tomography facility of the HMI. Nucl Instrum Methods Phys Res A. 2005;542:16–21.
9. Hilger A, et al. The new cold neutron radiography and tomography instrument CONRAD at HMI Berlin. Phys B. 2006;385–386:1213–5.

10. http://www.volumegraphics.com/.
11. Balek V, et al. Emanation thermal analysis and other radiometric emanation methods. In: Svehla G, editor. Wilson and Wilson's comprehensive analytical chemistry, Part XII. C. Amsterdam: Elsevier; 1984. p. 43–71.
12. Balek V, et al. Emanation thermal analysis. J Therm Anal Calorim. 2002;67:15–35.
13. Balek V. Emanation thermal analysis and its application potential. Thermochim Acta. 1991;192:1–17.
14. Beckman IN, et al. Theory of emanation thermal analysis: XI radon diffusion as the probe of microstructure changes in solids. J Therm Anal Calorim. 2002;67:49–61.
15. Ziegler JF, et al. The stopping and range of ions in solids. New York: Pergamon Press; 1985.